NASA TECHNICAL MEMORANDUM NASA TM-75160

FLUTTER ANALYSIS OF A GLIDER MADE OF SYNTHETIC MATERIALS

P.C. Hensing

(NASA-TM-75160) FLUTTER ANALYSIS OF A GLIDER MADE OF SYNTHETIC MATERIALS (National Aeronautics and Space Administration) 38 p HC A03/MF A01 CSCL 01A

N78-12012

Unclas
G3/02 53583

Translation of "Flutteranalyse van een kunststof zweefvliegtuig," Technische Hogeschool, Delft (Netherlands), Report VTH-187, Sept. 1974, 35 pages

NATIONAL AERONAUTICS AND SPACE ADMINISTRATION
WASHINGTON, D.C. 20546 OCTOBER 1977

TABLE OF CONTENTS

FLUTTER ANALYSIS OF A GLIDER MADE OF SYNTHETIC MATERIALS

P.C. Hensing
Delft Technical University

1. Introduction /3*

To aid in the certification of a glider, there are a number of requirements concerning, among other things, flutter behavior. The RLD-regulations require nonconstraint of flutter only up to 1.2 V_D. In practice, it was formerly sufficient when a number of rigidity criteria were satisfied. These criteria for rigidity are derived from empirical formulas and are reliable for gliders for which conventional constructions and materials are used. For the class of gliders now being developed, of which the "Standard Cirrus" is one, however, not only are other construction types and modern materials used, but at the same time a considerable improvement in performance has been made, among other things by the application of greater wing thinnesses. This all has a great influence on the flutter behavior, and it will be evident from what follows that the satisfying of rigidity criteria offers no guarantee of, for example, nonconstraint features of flutter. The first "Standard Cirrus," which was developed by the Amsterdam Glider Club (AGC) was one of the first gliders made of synthetic materials to be presented for certification in the Netherlands. It is, therefore, also clear that the RLD would not proceed to certification without further investigation.

Because the German authorities for airworthiness had adopted a more flexible attitude, the situation arose in which the "Standard Cirrus" had no certificate of airworthiness in Germany or in the Netherlands. Because it was not attractive to the German manufacturer, from the viewpoint

*Numbers in the margin indicate pagination in the foreign text.

of economy, to do a complete flutter investigation and because this economic aspect is also important for other foreign manufacturers, this would mean that the Dutch glider clubs could no longer pursue a course of furious development.

In order to break this impasse, an investigation of the vibration and flutter behavior of the "Standard Cirrus" was conducted, in consultation with the RLD, by the Under-department of Aircraft Construction at Delft TU. For this purpose, steady vibration tests were carried out on the AGC's equipment, which were used as a check of the calculated model. Then the tail vibration and flutter calculations were worked out on the IBM 360-65 computer at Delft TU. The unstationary air forces for the T-tail were calculated by the NLR. /4

Next, the direct determination of flutter behavior of the "Standard Cirrus" was attempted after seeing how far the results found are applicable to other gliders made of synthetic materials and if a simple method existed for making quantitative predictions on this subject.

2. Brief Description of the "Standard Cirrus"

The construction of the "Standard Cirrus," a glider of the standard class, is built almost entirely out of strengthened synthetic material. The wing was formed by means of a sandwich shell, consisting of two laminates of glass-fiber-reinforced synthetic resin and a core of solid foam. The bending rigidity was strengthened by means of a rib, which was up to 36% of the wing chord. This rib consists of a wooden bodypiece and couplings of glass rovings. The ailerons are not balanced. They are driven in by means of bars, which are laid in Teflon boxes. The rudders are each driven at one point into the end closest to the fuselage. The rudder chord is 23% of the wing chord.

The ballast tanks, each holding 30 liters, are found in the wing. These tanks are integrated into the wing construction and are found between the wing nose and the rib and are closed with two end-ribs.

The fuselage consists of a skin of glass-fiber-reinforced synthetic resin, strengthened with foam frames. The tail is made like a T-tail, whereby the horizontal tail surface acts as a shuttle rudder. This is almost completely balanced, while the direction rudder is fully balanced. The operation of the height rudder is separate, i.e. by rods, while the direction rudder mechanism from the service pedals to the rear of the cockpit consists of cables, from which the rods pass.

Figure 1 gives a sketch of the "Standard Cirrus"; in Table 1, a number of technical data are also mentioned.

3. Separation into Two Partial Systems: The Wing and the Rear Fuselage with the Tail Surfaces /5

For purposes of a simple description and to acquire a better overview, two separate systems are considered, namely the system in which the wing is flexible and the rest of the glider infinitely rigid, and the system in which the rear fuselage and the tail surfaces are flexible and the wing and front fuselage are infinitely rigid.

Because the amount of inertia as well as the air forces upon the wing are of an order greater than those on the tail surfaces, an interaction of both systems does not lie at hand, so that this approximation appears justified.

4. The Wing

4.1. Steady Vibration Investigation for the Wing

The quantities and basis upon which the flutter calculations are made (vibration eigen models and eigen frequencies in still air and the generalized masses) are determined for the purpose of the vibration calculations. These vibration calculations are made on the basis of an approximated mass and rigidity distribution.

In order to test the exactness of these approximations, the symmetric vibrations are calculated, moreover, for the case in which the fuselage is considered unstressed. At the same time, steady vibration measurements are made for this configuration. The comparison of the calculation and the experiment gives good agreement, so that there is no doubt of the reliability of the output data.

The determination of the aileron's moment of inertia deserves separate mention. It is obvious that this quantity plays an important role in the mechanism of flutter. The moment of inertia of the control system must also be considered in the aileron moment of inertia. Also herewith is derived a determination of the mass distribution and of the displacements of the various parts which is as exact as possible. The results of the experimental calculation of this quantity for the purpose of a vibration test must be viewed with proper suspicion, because the dry friction which is present in the control circuit makes the eigen frequency /6 dependent on the thrust amplitude.

The vibration calculations for the free (not unstressed) glider are made for both symmetric and time-symmetric vibration models. The results are reproduced in Figs. 2 and 3.

4.2. Discussion of the Steady Vibration Behavior of the Wing

Figures 2 and 3 give the amplitudes for an average number of wings for different eigen vibration models. To distinguish positive and negative amplitudes, crosshatching and blackening are used as indications.

In studying the results of the steady vibration investigation, the large difference between the bending and torsion frequencies attracts one's attention, while the mass coupling between the bending and torsion is slight. Thus, the first three symmetric eigen vibration models practically alone make up the bending (the fundamental and the second overtone of symmetric bending), while the fourth eigen vibration practically alone makes up the torsion.

For the asymmetric eigen vibration models, it is felt that the first two eigen vibration models can be described practically alone by the fundamental and the first overtone of asymmetric bending, while the third eigen vibration model is identical with the fourth symmetric eigen vibration model and comprises torsion principally. This steady vibration behavior is characteristic of the modern class of gliders made of synthetics and is determined for flutter behavior.

The presence of water ballast appears to have hardly any effect on the eigen vibration models. In the flutter calculation, it will always come from the eigen vibration models of the configuration without ballast. The eigen frequencies and the generalized masses have values which are quite deviant for the configuration with ballast.

The generalized masses can be calculated from the eigen vibration models found and the estimated mass data (see Figs. 2 and 3 and Table 2).

4.3. Flutter Calculation for the Wing

/7

The flutter equations were derived in the usual way, by the Rayleigh-Ritz method. Herewith the transformation constructed was considered from a number of assumed transformation functions; thus:

$$\phi(y,t) = \sum_{i=1}^{n} \phi_i(y)\, q_i(t)$$

Here $\phi_i(y)$ are the transformation functions and $q_i(t)$ the (time-dependent) mixed factors, with generalized coordinates assumed.

For these transformation functions, the calculated orthogonal vibration models were assumed, completed with the "rigid body modes" of interest here and equally the rudder motion (see Table 4).

The flutter equations are therefore:

$$\sum_{j=1}^{n} U_{ij}\, \ddot{q}_j + \nu_i^2\, (1+ig) U_{ii} q_i = -\nu^2 \sum_{j=1}^{n} L_{ij} q_j \quad (i = 1, \ldots, n)$$

Here the generalized masses are:

$$U_{ij} = \int_0^b \phi_i \phi_j\, m(y)\, dy$$

and L_{ij}, the generalized air forces. g is a fictitious damping, which must be added in order to make the harmonic system vibrate (in the figures, the letter h is used for this.)

The present structural damping was neglected in the calculations. The generalized air forces were calculated by means of the well-known strip theory for an incompressible, frictionless flow. H is:

$$L_{ij} = L_{ij}^{hh} + L_{ij}^{\alpha\alpha} + L_{ij}^{\beta\beta} + L_{ij}^{h\alpha} + L_{ij}^{\alpha h} + L_{ij}^{h\beta} + L_{ij}^{\beta h} + L_{ij}^{\alpha\beta} + L_{ij}^{\beta\alpha}$$

Here, this is:

$$L_{ij}^{hh} = \int_0^b m_L \frac{k_a}{\omega^2} h_i h_j \, dy$$

$$L_{ij}^{\alpha\alpha} = \int_0^b m_L \frac{m_b}{\omega^2} \alpha_i \alpha_j \ell^2 \, dy$$

$$L_{ij}^{\beta\beta} = \int_0^b m_L \frac{n_c}{\omega^2} \beta_i \beta_j \ell^2 \, dy$$

$$L_{ij}^{h\alpha} = \int_0^b m_L \frac{k_b}{\omega^2} h_i \alpha_j \ell \, dy$$

$$L_{ij}^{\alpha h} = \int_0^b m_L \frac{m_a}{\omega^2} \alpha_i h_j \ell \, dy$$

$$L_{ij}^{h\beta} = \int_0^b m_L \frac{k_c}{\omega^2} h_i \beta_j \ell \, dy$$

$$L_{ij}^{\beta h} = \int_0^b m_L \frac{n_a}{\omega^2} \beta_i h_j \ell \, dy$$

$$L_{ij}^{\alpha\beta} = \int_0^b m_L \frac{m_c}{\omega^2} \alpha_i \beta_j \ell^2 \, dy$$

$$L_{ij}^{\beta\alpha} = \int_0^b m_L \frac{n_b}{\omega^2} \beta_i \alpha_j \ell^2 \, dy$$

The functions k_a, k_b, k_c, m_a, m_b, m_c, n_a, n_b, and n_c are taken from references 2 and 3.

$m_L = \pi p l^2$

p = air volume

l = half-chord

b = half-span

h_i = vertical translation of the quarter-chord point for the i-th transformation function

α_i = rotation about the quarter-chord line for the i-th transformation function /9

β_i = rudder angle for the i-th transformation function

4.4. Description of the Flutter Behavior of the Wing

For the calculation of the symmetric behavior, it is derived from the vibration models 2 through 5, and at the same time a "rigid body mode" was taken for the calculation, i.e. the vertical translation of the fuselage. Figures 4 and 5 show the course of the damping and the eigen frequency, respectively, with the speed for the various eigen vibration models. The samping of branch 4 appears to change signs at 117 m/sec, and this branch is therefore flutter-prone. In considering the vibration models, flutter appears to develop through the interaction of the second bending vibrations and the first torsion vibration. The eigen vibration model belonging to branch 5 at v=0 was characterized by torsion, while branches 2, 3, and 4 were characterized by the first, second and third vibration models of bending, respectively. From ±70 m/sec, branch 4 was, through interaction with branch 5, characterized by torsion, so that the flutter type at 117 m/sec can be characterized as bending-torsion flutter. The speed at which this appears is considerably higher than 1.2 V_D (see Table 1), so that there is, in the symmetric case, a considerable margin of safety, as far as wing flutter is concerned. The presence of water ballast hardly appears to introduce any danger of flutter, so that in the following, considerable attention will be given especially to asymmetrical flutter behavior.

The antisymmetric flutter calculations were done for a system with 5 degrees of freedom, i.e. the rolling motion of the fuselage, the aileron output, and the vibration models 8 through 10. From Figures 6 and 7, it appears that two potential flutter

possibilities are present, i.e, branches 8 and 9. This leads hereby to an interaction of the first and second bending-rudder vibrations.

In the asymmetric case, the aileron frequency appears to increase practically linearly from 0 cps. When the eigen frequency in motionless air is greater than 0 cps (such as in the symmetric case), the frequency branch appears to approach this linear ratio asymptotically. That such a behavior is to be expected may be evident from the following: /10

The equation of motion for the aileron is:

$$(U_{22} - L_{22})\, q_2 = \frac{\nu_2^2}{\nu^2} U_{22} (1 + ih)\, q_2 \qquad (1)$$

where

U_{22} = the generalized mass of the rudder

L_{22} = the generalized air force at the rudder
($L_{22} = L_{22}' + iL_{22}''$)

ν_2 = eigen frequency of the aileron in motionless air

ν = eigen frequency of the aileron

h = damping

q_2 = generalized coordinate

$i = \sqrt{-1}$

Thus:

$$\frac{\nu_2^2}{\nu^2} = \frac{U_{22} - L_{22}' - hL_{22}''}{U_{22}(1 + h^2)} \qquad (2)$$

And if $h = 0$:

$$\nu = \nu_2 \sqrt{\frac{U_{22}}{U_{22} - L_{22}}} \qquad (3)$$

When the term $U_{22} - L_{22}$ is negative, the expression for ν has no

significance. Thus:

$$U_{22} - L_{22}' = I_r \beta^2 - \pi\rho\ell^4 \frac{n_c'}{\omega^2} \beta^2 b_r > 0 \qquad (4)$$

Here:

I_r = moment of inertia of the aileron about the rudder
β = size of the rudder result
ρ = air density
ℓ reference length
n'_c = coefficient of air power /11
ω = reduced frequency:
b_r = width of the rudder

Now n'_c is practically constant for the area of ω considered, such that

$$\omega > \sqrt{\frac{\pi\rho\ell^4 n_c' b_r}{I_r}} \qquad (5)$$

For ω values which are smaller, there is no longer a real loss for ν, so that the agreement of the asymptote upon approximation is

$$V = \nu \sqrt{\frac{I_r}{\pi\rho\ell^2 n_c' b_r}} \qquad (6)$$

From the above, it appears that the frequency of the aileron increases practically linearly with an increase in velocity, while the bending frequency remains constant. This gives rise to the already previously mentioned two critical cases (branches 8 and 9).

From expression 6, it appears that the greater the aileron moment of inertia, the greater the steepness of the asymptote, so that interaction with the bending branches occurs for cases with a higher velocity (see also Fig. 12). An accurate determination of the aileron moment of inertia (including the steering mechanism) is thus required. One must pay strict attention to the moment of inertia for the steering mechanism, which determines to a significant degree the size of the aileron moment of inertia.

In the symmetric case, the dangerous case of flutter outlined above does not occur, because in this case the aileron frequency in still air does not amount to 0 cps, but it is higher than the bending frequency caused.

4.5 The Effect of the Presence of Ballast

In Figs. 6 and 7, a comparison is presented for antisymmetric behavior with and without ballast. From this, it appears that the differences are insignificant. When the ballast tanks /12 are filled, V_D is higher, however (i.e. 78.9 m/sec; without ballast, 74.7 m/sec), so that for these configurations, somewhat more severe requirements are set. The discussion of flutter behavior will also be limited to the antisymmetric behavior of the configuration with water ballast.

4.6 Quantities Determined for Flutter Behavior for the Configuration Measured

From the foregoing, it appears that antisymmetric behavior of the configuration with water ballast is measured. In the following, the case will be taken up in which special attention will be paid to the quantities which have a direct effect on the size of the critical velocity.

In Figs. 6 and 7, results were presented for flutter calculations for a calculation model with five degrees of freedom. It appears that the interaction between the first bending vibration and the rudder vibration and that between the second bending vibration and the rudder vibration can be approximated in an adequate way by binary calculation models. A comparison of the flutter calculations for the calculation model with five degrees of freedom and the results of the two calculations for binary systems with two degrees of freedom (the first and second bending/rudder vibrations, respectively) are presented in Figs. 8 and 9.

The danger of flutter is determined by means of the following factors:

1) Interaction of the two bending vibrations and the rudder vibration causes a rapid return in damping of the second bending vibration, which gives rise to flutter. The question now is whether this behavior occurs above or below 1.2 V_D.

2) Damping of the first bending vibration is smaller in absolute value in a specific velocity region and can change sign in certain cases. The velocity region in which it occurs lies in any case below 1.2 V_D (between 40 and 60 m/sec). The question is, by means of which factor is this behavior determined and if a satisfactorily large margin of safety is present in the "Standard Cirrus."

The size of the velocity at which damping of the second bend- /13
ing vibration changes sign is defined by the slope of the frequency characteristic of rudder vibration. As this characteristic becomes steeper, interaction between rudder vibration and the second bending vibration takes place at a higher rate.

From Section 4.4, it appears that the slope of the frequency characteristic is defined by the size of the aileron moment of inertia. For the "Standard Cirrus," flutter of the second bending vibration appears to occur at 114 m/sec, which is considerably higher than 1.2 V_D (94.7 m/sec), so that this flutter possibility causes no danger for the "Standard Cirrus."

In the foregoing, calculations for flutter were discussed originating from structural damping and dry friction in the steering mechanism. In considering the interaction of the first bending vibration and rudder vibration, there develops with this assumption an all too unfavorable picture. In this case, this also results from a normally present structural damping of 0.05 and dry friction, which are derived from the measurements from reference 5. From Fig. 10, it appears that a definite margin of safety is present.

The means by which damping of the eigen vibration form 8 returns in the velocity region of 40 to 60 m/sec is dependent on the size of the static moment of the aileron, the size of the aileron moment of inertia, and the amount of dry friction in the steering mechanism. As appears from Fig. 11, flutter behavior is not as sensitive to small changes in the friction present in the steering system. A 40% reduction in friction force still has no detrimental results.

With an increase in the aileron moment of inertia, the velocity at which damping returns, corresponding to that stated in Section 4.4, appears to increase (see Fig. 12). At the same time, the behavior appears to be more flutter-critical as the aileron moment of inertia increases. Actual danger of flutter exists with a 40% increase in aileron moment of inertia, so that it can be said that flutter behavior also is not sensitive to samll changes in the aileron moment of inertia. /14

Fig. 13 shows the effect of the size of the aileron's static moment. Variations in this static moment appear to be directly affected by flutter behavior. The present margin of safety is 12%.

In the above, the moment of inertia and static moment of the aileron were varied separately. In practice, however, a change in the static moment (such as that due to carrying extra mass), at

the same time causes a change in the moment of inertia, so that it is required, on a figure, to read which combinations of I and S give rise to stable or unstable behavior (see Fig. 14).

4.7 Conclusions and Evaluation of the Flutter Behavior Found for the Wing

From the foregoing, it appears that with regard to the structural damping and dry friction present in the aileron steering system, the wing of the "Standard Cirrus" is flutter-free in the required velocity region (up to 1.2 V_D).

Two possible critical situations are distinguished for the configuration with the joystick released, i.e. interaction between the first antisymmetric bending vibration and the aileron motion and interaction between the second antisymmetric bending vibration and the aielron motion. Both situations are not critical for the "Standard Cirrus," but they can be critical for aircraft of similar construction in which somewhat different mass and rigidity are present. Such flutter types, such as the formerly used rigidity criteria, are not understood (there is no criterion for the bending rigidity of the wing).

In the "Standard Cirrus," for a good prediction of flutter behavior of the wing, it appears satisfactory to make two flutter calculations for a system with two degrees of freedom (the system with the first antisymmetric bending vibration form and aileron /15
motion as degrees of freedom and the system with the second antisymmetric bending vibration form and aileron motion as degrees of freedom; see Figs. 11 and 12).

In addition, for other synthetic gliders, these two calculations are sufficient, provided that the wind construction is comparable to that of the "Standard Cirrus."

This can be derived from the steady vibration behavior. Small differences which show up in the geometry may hereby be ignored.

Well-known examples are the SB 9 and the ASW 15B (see references 6 and 7). The SB 9 has a larger span than the "Standard Cirrus". The eigen frequencies and also the critical speeds are therefore lower.

The SB 9 shows both the above-described critical conditions and flutters at 90 kmph with a frequency of 3.3 cps and at 140 kmph with a frequency of 5.8 cps.

In addition, the calculations for the ASW 1513 show such a picture. The interaction between the second asymmetrical bending vibration and the aileron motion yields flutter at 455 kmph. The first critical case is not established for these calculations because the aileron frequency in motionless air is taken to be higher than the eigen frequency of the first asymmetrical bending vibration.

Mass balancing of the ailerons will have control for any type up to the elimination of the danger of wing-rudder flutter.

5. The Rear Fuselage with Tail Surfaces

5.1. The Steady Vibration Investigation of the Tail and Discussion of the Steady Vibration Behavior

The steady vibration investigation for the tail has been limited to the following considerations of the asymmetric behavior. The symmetric behavior was determined by means of the following degrees of freedom: vertical bending of the rear fuselage, bending and torsion of the stabilo, and the stabilo -- "pitch" (height rudder) motion. The eigen frequencies of the stabilo bending and stabilo torsion vibration are so high (higher than 20 cps) that these degrees of freedom are not of interest. Interaction of the vertical /16
fuselage bending and the height rudder output is hardly possible

because the height rudder is almost completely unbalanced. All this makes it implausible for symmetric vibration models to be able to cause flutter.

Asymmetric behavior, on the other hand, makes flutter more of a possibility. In this case, the degrees of freedom are: horizontal bending and torsion of the rear fuselage, rolling and yawing of the stabilo due to the deformation of the fixed fittings, bending and torsion of the fin and the direction rudder output. Bending and torsion of the fin appear to have eigen frequencies too high to be able to produce any danger. The steady vibration investigation has been directed toward the remaining vibration models and eigen frequencies. As in the steady vibration, investigation of the wing, here calculations as well as measurements were also made.

In the flutter calculations, they are derived from the measured eigen vibrations models 14 and 15 (see Figure 15 and the description in Table 5). The remaining degrees of freedom, i.e. rolling and yawing of the stabilo and the direction rudder output as "artificial modes" assumed for the calculation (see Table 5).

For the calculation of the generalized masses, use is made of the mass data in Table 3.

5.2. Determination and Discussion of the Flutter Behavior of the Tail

As in the determination of flutter behavior for the wing, use is also made for the tail of the Rayleigh-Ritz method. It is derived from the transformation functions which are given in Table 5.

For the calculation of the air forces, the use of strip theory can lead to a large deviation, because for the T-tail, it is no longer a question of thin drag surfaces; at the same time, moreover, the interference of the stabilo and fin play some role. For calculating the generalized air forces, therefore, use is made of the

doublet lattice method, as described in reference 4. The air-force calculations were worked out on the NLR. The results of the flutter calculations are presented in Figures 16 and 17. From this, it appears that at speeds lower than 1.2 V_D, the critical conditions are not satisfied. This results in a lag in the line of expectation. Possible causes of flutter could be the interaction of vibration model 14 or 15 with the direction-rudder motion. The direction rudder is, however, completely unbalanced, so that these possibilities must be considered out of the question. /17

5.3. Conclusions and Evaluation of the Flutter Behavior Found for the Tail

From para. 5.1., it appears that flutter due to the interaction of symmetric eigen vibration models of the tail can be considered a priori an impossibility.

The asymmetric eigen vibration models, on the other hand, present a range of possibilities. The flutter calculations show that in this case also there is no danger of flutter at velocities below 1.2 V_D, which is explainable on the basis of the high rigidity of the fin and the balancing of the direction rudder.

In the discussion of the wing, it can be said that for modern gliders made of synthetic materials, the wing constructions used are similar, so that the possible flutter types are also identical.

The same cannot be said of the tail. Here, among other things, no predictions can be made for the tail for the measured flutter type, so that the flutter calculations cannot be simplified a priori.

REFERENCES

1. Bisplinghoff, R.L., H. Ashley and R.L. Halfman, Aeroelasticity, Addison-Wesley, 1955.

2. Theodorsen, T., "General theory of aerodynamic instability and the mechanism of flutter," Report 496, NASA.

3. Küssner, H.G. and L. Schwartz, "The vibrating wing with aerodynamically balanced rudder," Luftfahrtforschung 17 (1940).

4. Roos, R. and R.J. Zwaan, "Calculation of instationary pressure distributions and generalized forces with the doublet lattice method," TR 72037 U, NLR.

5. Stender, W., "Estimation of flutter possibility in the 'Standard Cirrus' Sailplane," Report dd. 22-12-1969.

6. Niedbal, N., "Flutter analysis of the ASW 15B sailplane, under conditions of measured vibration characteristics," Report No. IB 253-73 J 01, DFVLR, March 1973.

7. Zacher, H., "Aileron-influenced bending flutters in a sailplane Aero-Revue 93 (February 1974).

TABLE 1: TECHNICAL DATA FOR THE "STANDARD CIRRUS" /19

Geometry

Wing span	15.0 m
Wing surface area	10.0 m^2
Thinness	22.5
Fuselage length	6.35 m
Fuselage height in cockpit	0.83 m
Fuselage width in cockpit	0.62 m
Span of stabilo	2.40 m

Weight

Empty weight	202 kg
Max. weight for takeoff without ballast	330 kg
Max. weight for takeoff with ballast	390 kg

Performance

Max. permissible flight speed, V_{NE}	61.1 m/sec	220 kmph
V_D (according to OSTIV) without ballast	74.7 m/sec	269 kmph
V_D with ballast	78.9 m/sec	284 kmph
Stall speed	17.2 m/sec	62 kmph
Min. descent rate at 70 kmph	0.57 m/sec	
Best glide number at 80 kmph	38	

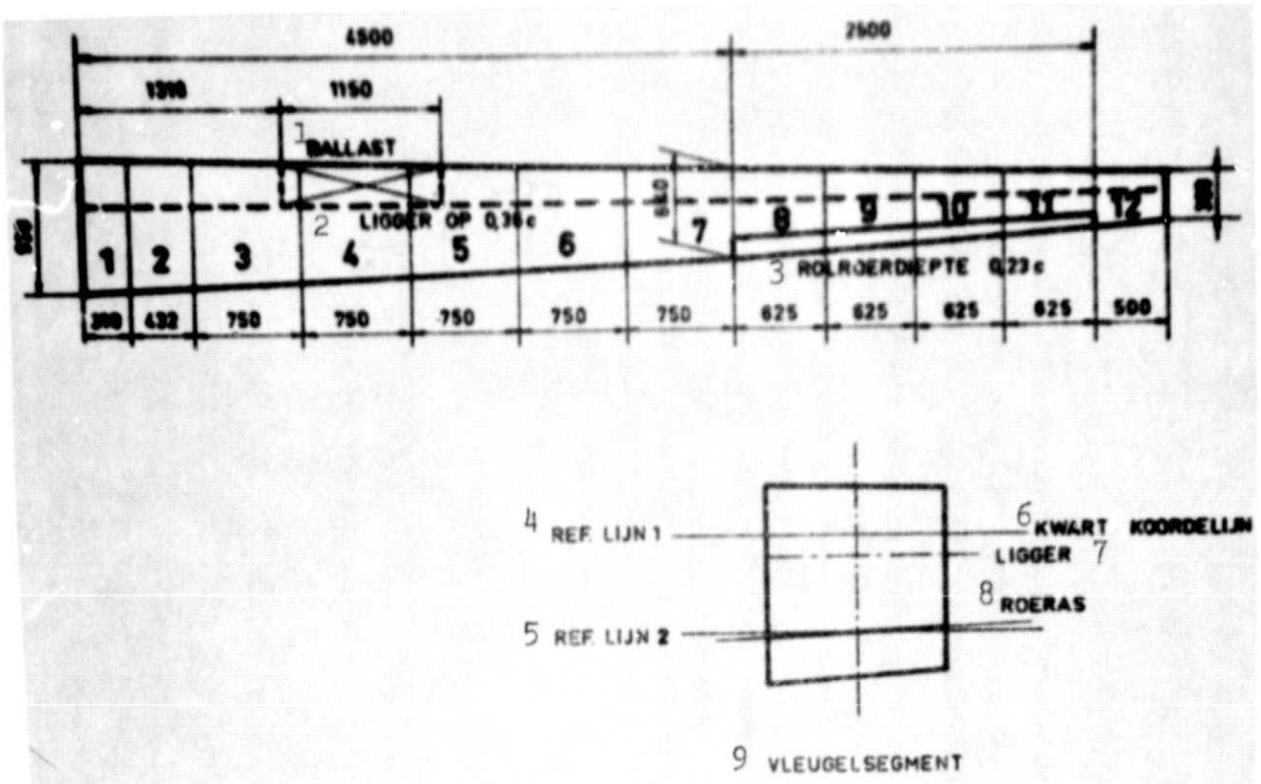

Key:
1. Ballast
2. Lies up
3. Aileron depth
4. Ref. line 1
5. Ref. line 2
6. Quarter chord line
7. Layer
8. Rudders
9. Wing segment

TABLE 2: MASS DATA FOR THE WING

	1	2	3	4	5	6	7	8	9	10	11	12
m	0,306	0,950	(1,111) 0,778	(2,750) 0,666	(1,331) 0,692	0,575	0,443	0,321	0,276	0,246	0,201	0,153
S_1	0,0306	0,1175	(0,0912) 0,0980	(0,0398) 0,0819	(0,0739) 0,0866	0,0690	0,0495	0,0359	0,0287	0,0219	0,0152	0,0076
I_1	0,0039	0,0471	(0,0452) 0,0432	(0,0469) 0,0344	(0,0310) 0,0272	0,0205	0,0177	0,0116	0,0087	0,0061	0,0038	0,0019
S_2	-	-	-	-	-	-	-	0,00360	0,00279	0,00221	0,00158	-
I_2	-	-	-	-	-	-	-	0,00122	0,00085	0,00059	0,00037	-

m = mass (kg sec^2/m)

I = moment of inertia (km sec^2 m)

S = static moment (kg sec^2)

Index 1: with respect to ref. line 1

Index 2: with respect ot ref. line 2

In parentheses are numbers for filled ballast tanks.

TABLE 3: MASS DATA FOR THE TAIL /21

Key on following page.

Key: 1. Mass (kg sec^2/m)

2. Moment of inertia about the X1-axis (kg sec^2 m)

3. Moment of inertia for fin + direction rudder about ref. line 1 (kg sec^2 m)

4. Moment of inertia of direction rudder about ref. line 2 (kg sec^2 m)

5. Static moment of fin + direction rudder about ref. line 1 (kg sec^2)

6. Static moment of direction rudder about ref. line 2 (kg sec^2)

7. a) Moment of inertia of the stabilo about the X2 axis

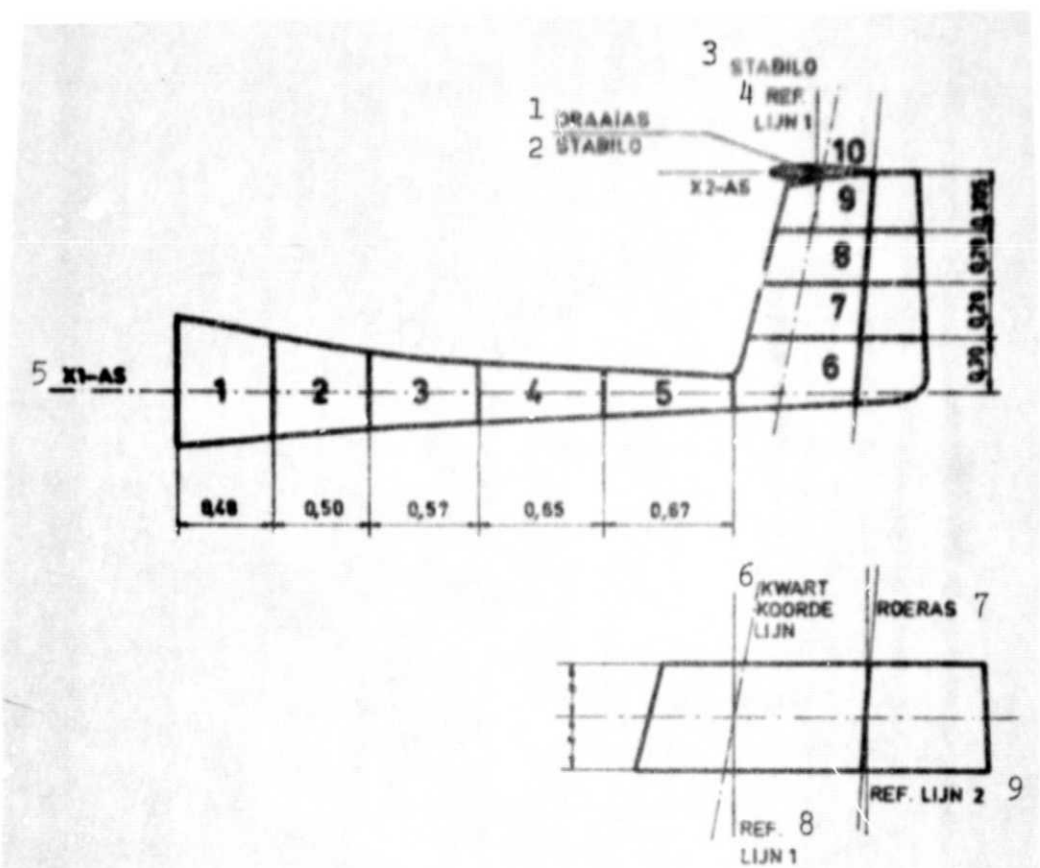

Key: 1. Bends 2. Stabilo 3. Stabilo 4. Ref. line 1 5. X1 axis
6. Quarter chord line 7. Ref. line 1 8. Rudders
9. Ref. line 2

TABLE 4. SUMMARY OF THE TRANSFORMATION FUNCTIONS USED IN THE FLUTTER CALCULATIONS FOR THE WING /22

no	symm. asymm.	characteristics of the transformation function	eigenfreq. (rad s^{-1})	
			without ballast	with ballast
1	S	vertical translation	0	
2	S	fundamental bending	16.3	
3	S	first overtone bending	60.1	
4	S	second overtone bending	143.9	
5	S	fundamental torsion	185.7	
6	A	rolling	0	0
7	A	rudder motion	0	0
8	A	fundamental bending	44.1	38.3
9	S	first overtone bending	125.2	115.6
10	A	fundamental torsion	185.7	171.5

TABLE 5. SUMMARY OF THE TRANSFORMATION FUNCTIONS USED IN THE FLUTTER CALCULATIONS OF THE TAIL /23

no.	characteristics of the transformation function	eigenfreq. (rad s^{-1})
11	rolling	0
12	yawing	0
13	motion of the direction rudder	0
14	horizontal bending of the rear fuselage coupled with torsion of the rear fuselage	31.2
15	torsion of the rear fuselage coupled with horizontal bending of the rear fuselage	61.6
16	yawing of the stabilo	75.4
17	rolling of the stabilo	125.7

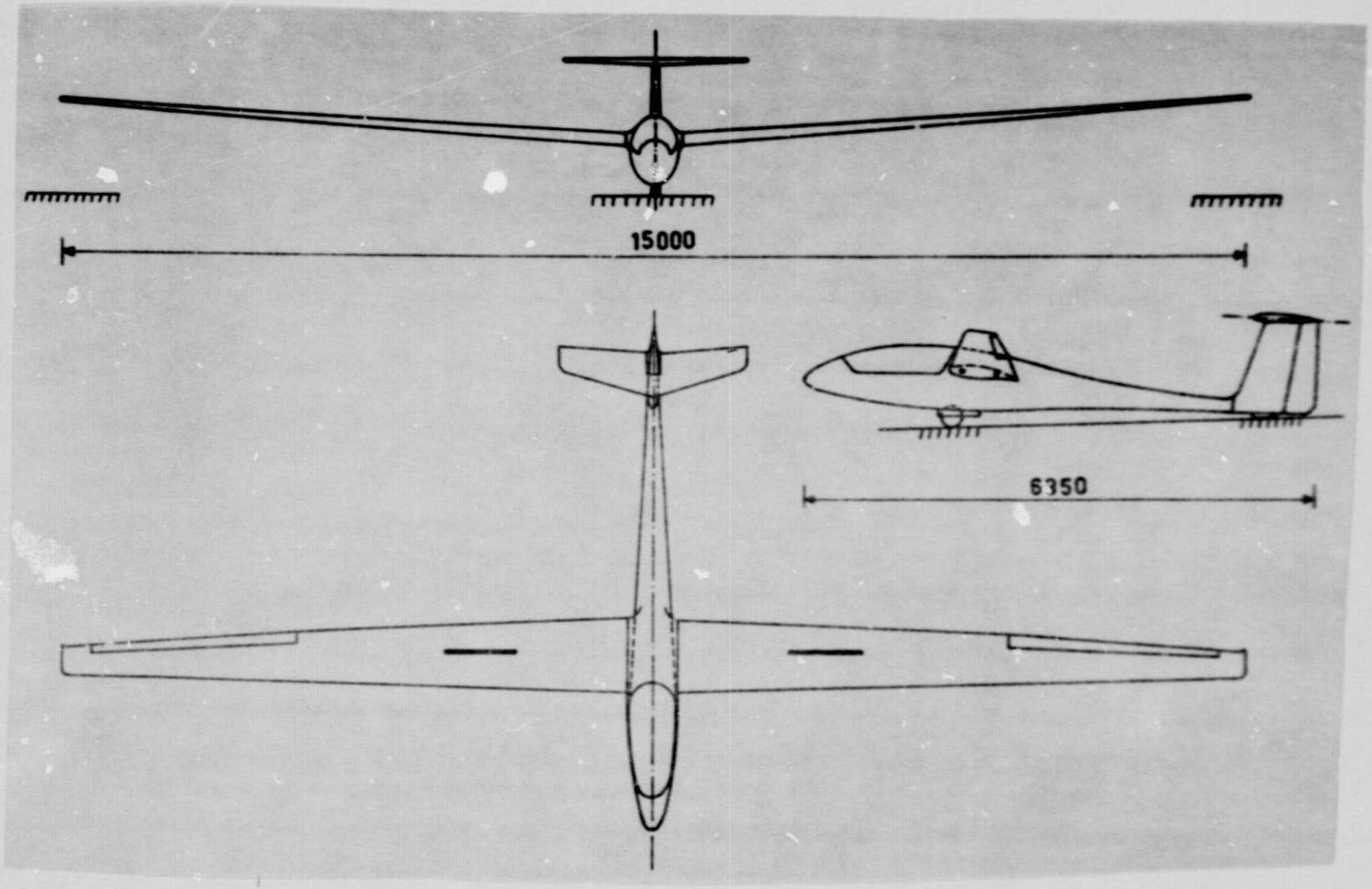

Fig. 1. Sketch to scale of the "Standard Cirrus."

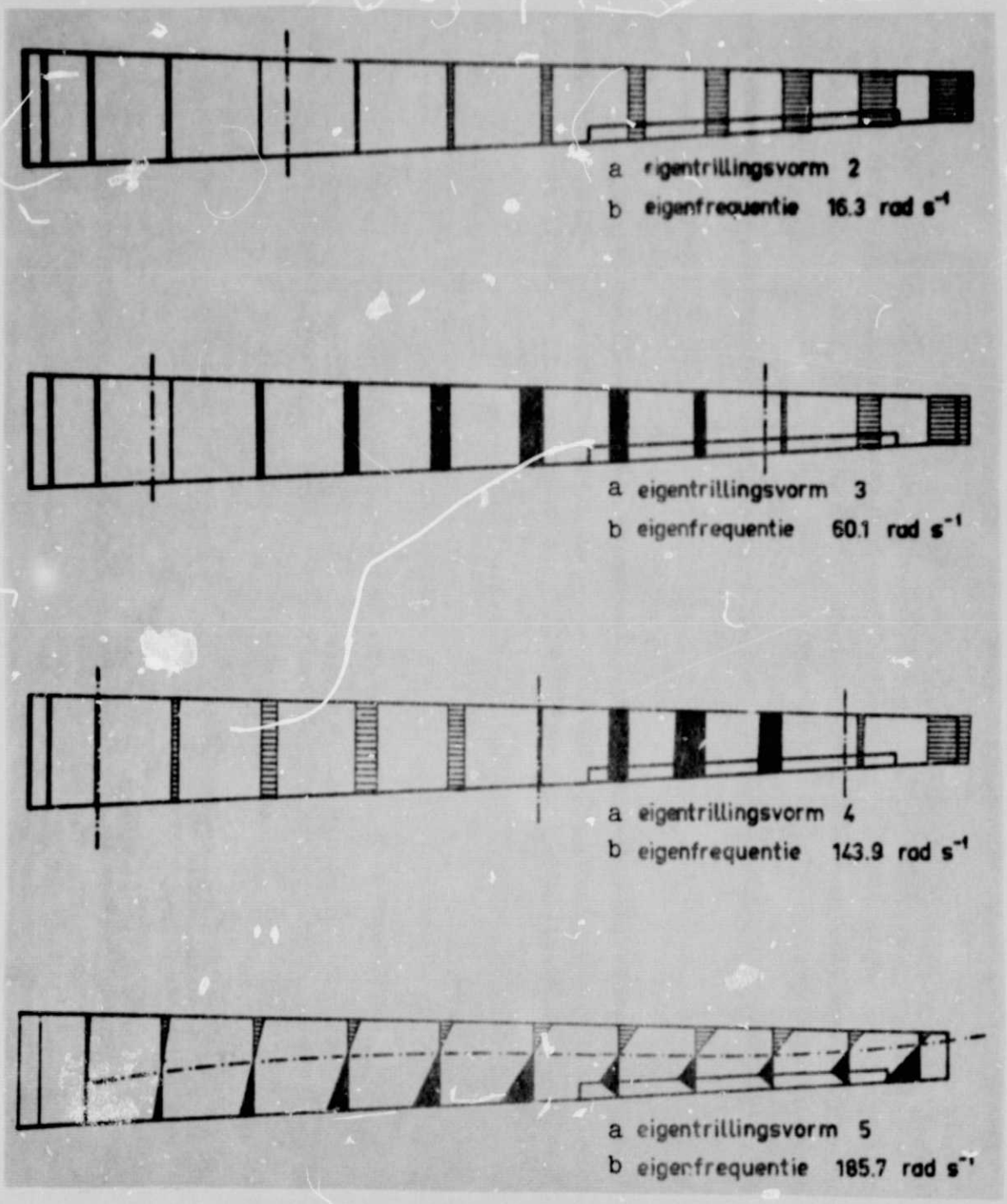

Fig. 2. Symmetrical eigen vibration models of the wing (eigen frequencies without ballast).

Key: a. Eigen vibration model
b. Eigen frequency

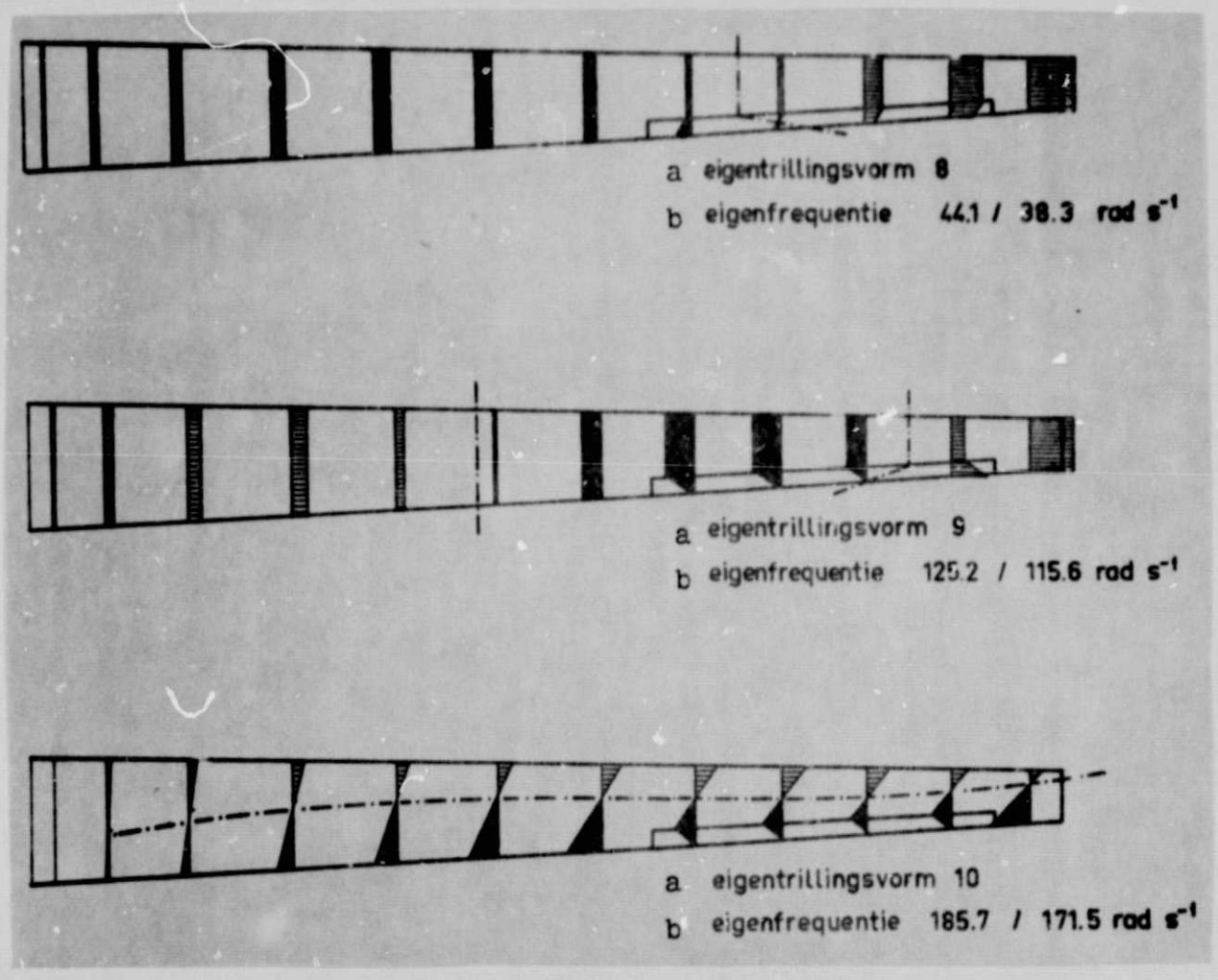

Fig. 3. Asymmetrical vibration models of the wing (eigen frequencies without ballast / with ballast)

Key: a. Eigen vibration model
b. Eigen frequency

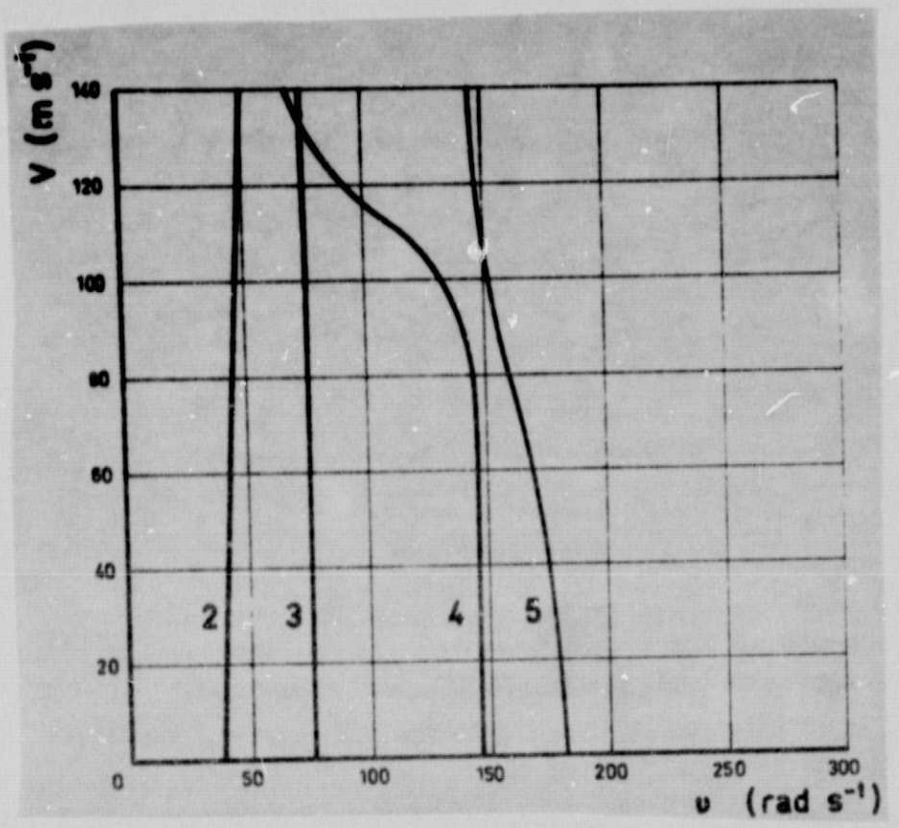

Fig. 4. Relationship between flight speed V and eigen frequency υ; symmetric eigen vibration models, without ballast.

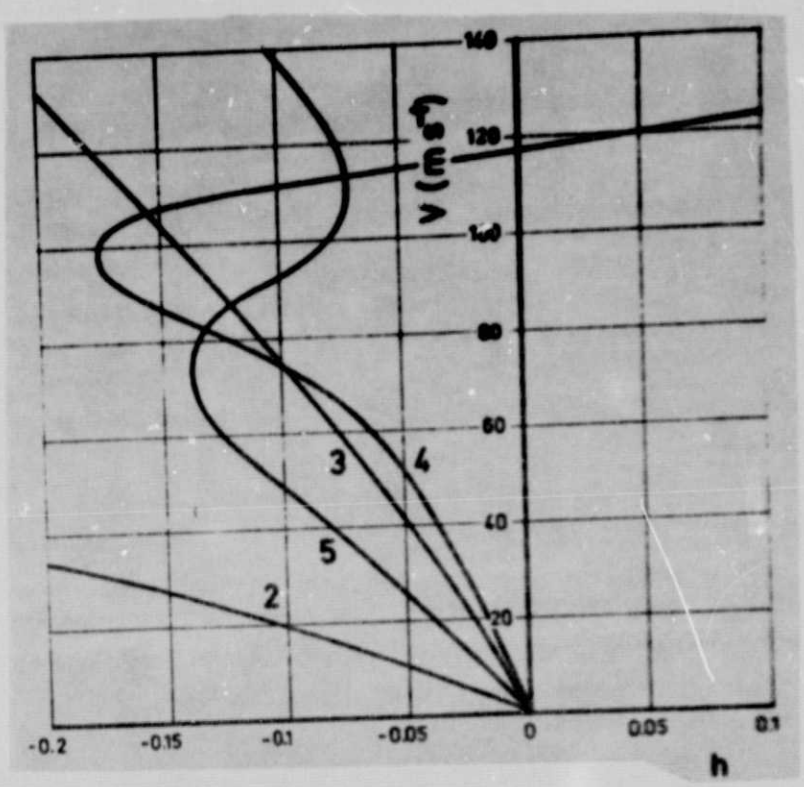

Fig. 5. Relationship between flight speed V and the damping factor h; symmetric eigen transformation models, without ballast.

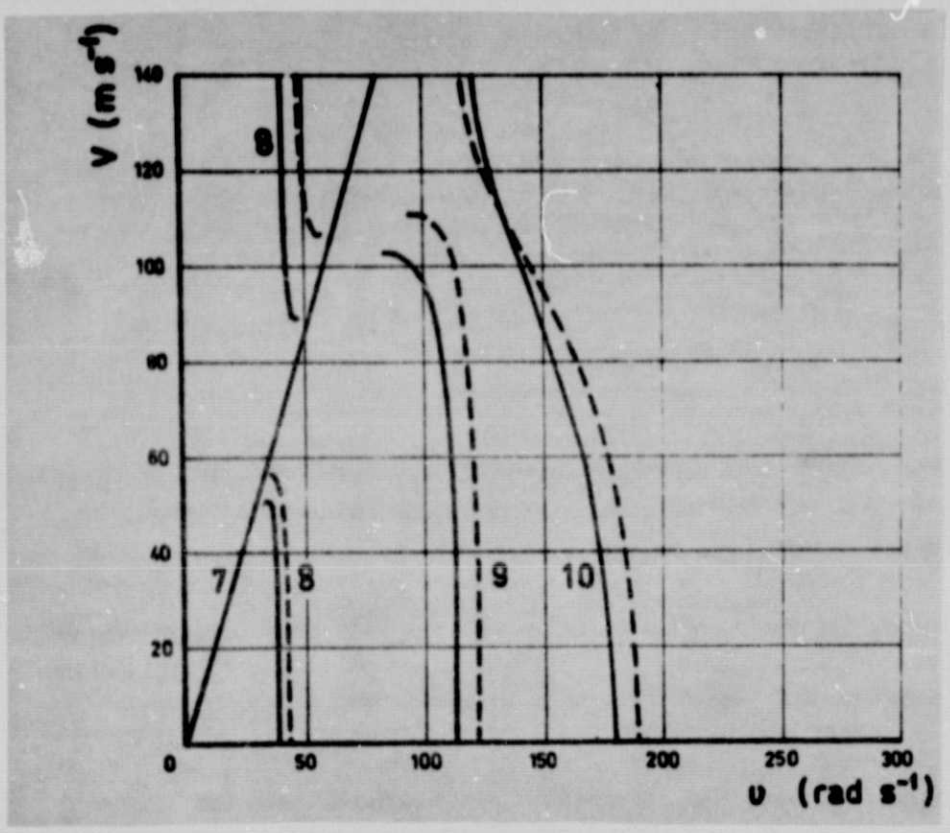

Fig. 6. Relationship between flight speed V and the eigen frequency ν; asymmetrical eigen vibration models.

—— with ballast

---- without ballast

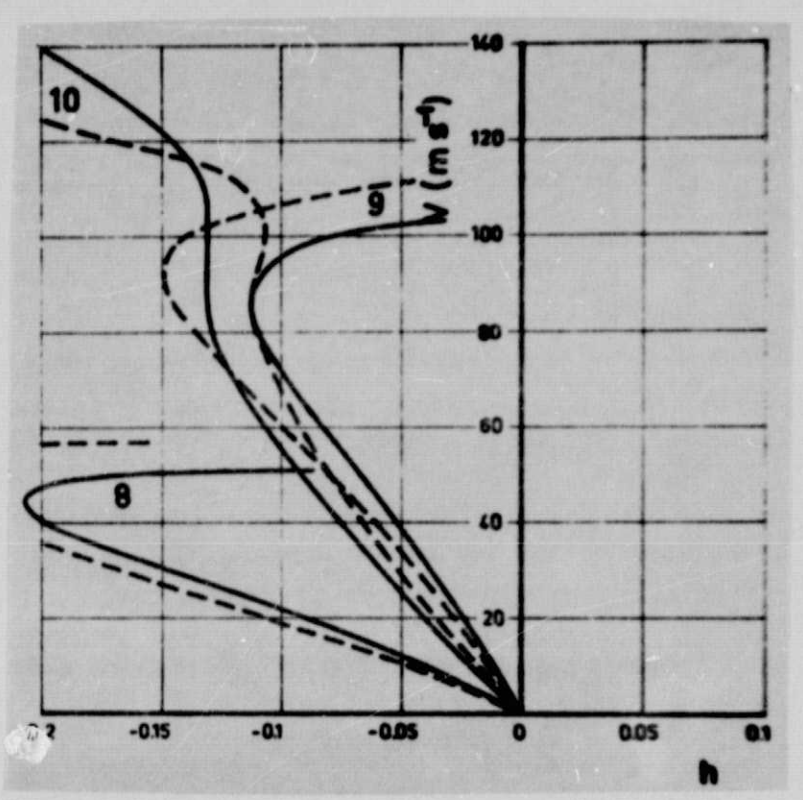

Fig. 7. Relationship between flight speed V and the damping factor h; asymmetrical eigen vibration models.

—— with ballast

---- without ballast

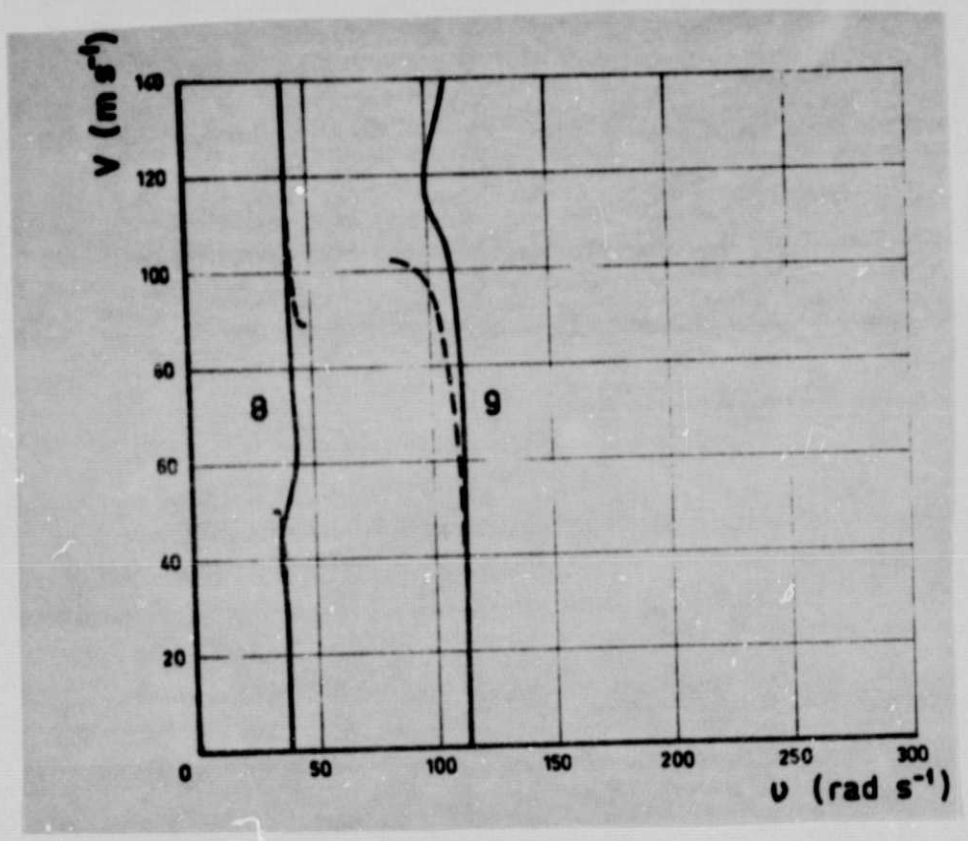

Fig. 8. Curve of the eigen frequency with the flight speed for eigen vibration models 8 and 9 for different calculated models, with ballast.

—— results for binary flutter calculations

---- calculated model with 5 degrees of freedom

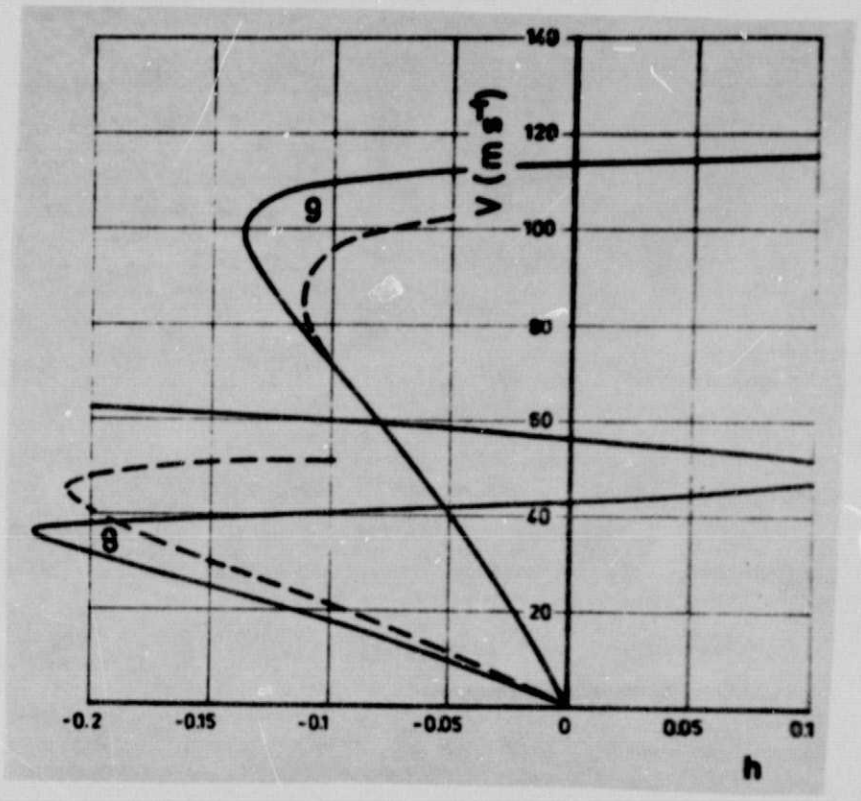

Fig. 9. Curve of damping with the flight speed for eigen vibration models 8 and 9 for different calculated models, with ballast.

—— results for binary flutter calculations

---- calculated model with 5 degrees of freedom

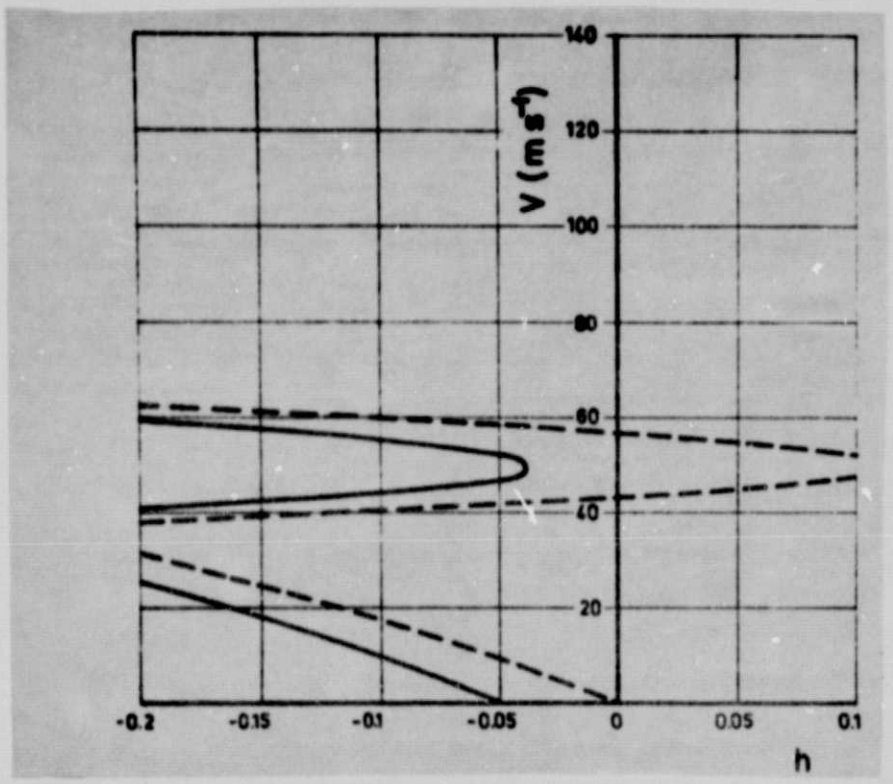

Fig. 10. Damping characteristics for eigen vibration model 8, with ballast.

—— with reference to structural damping and dry friction

---- without damping or friction

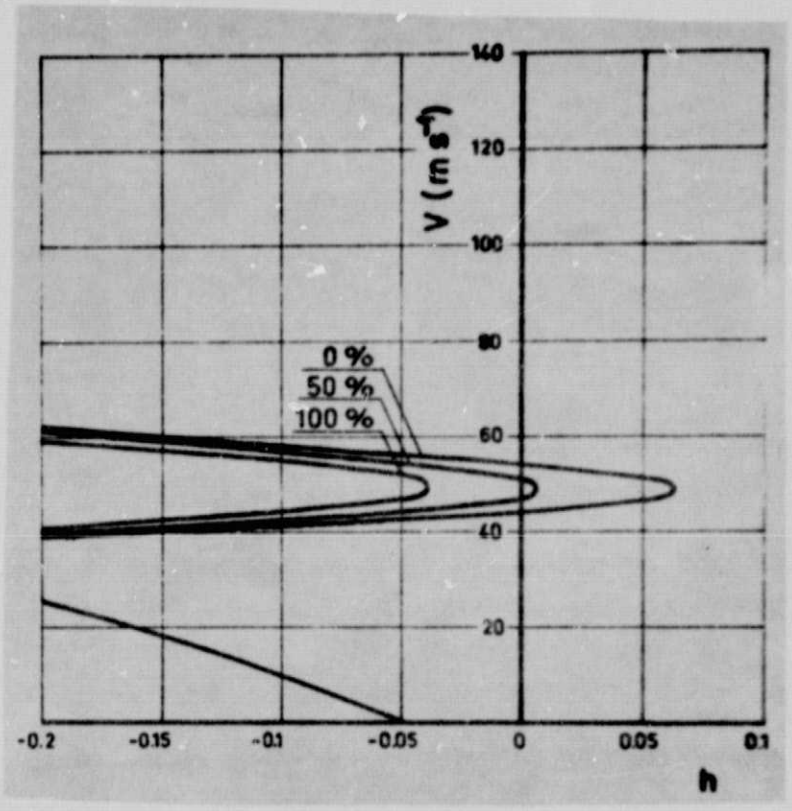

Fig. 11. Damping characteristics for eigen vibration model 8 for different values of dry friction, with ballast.

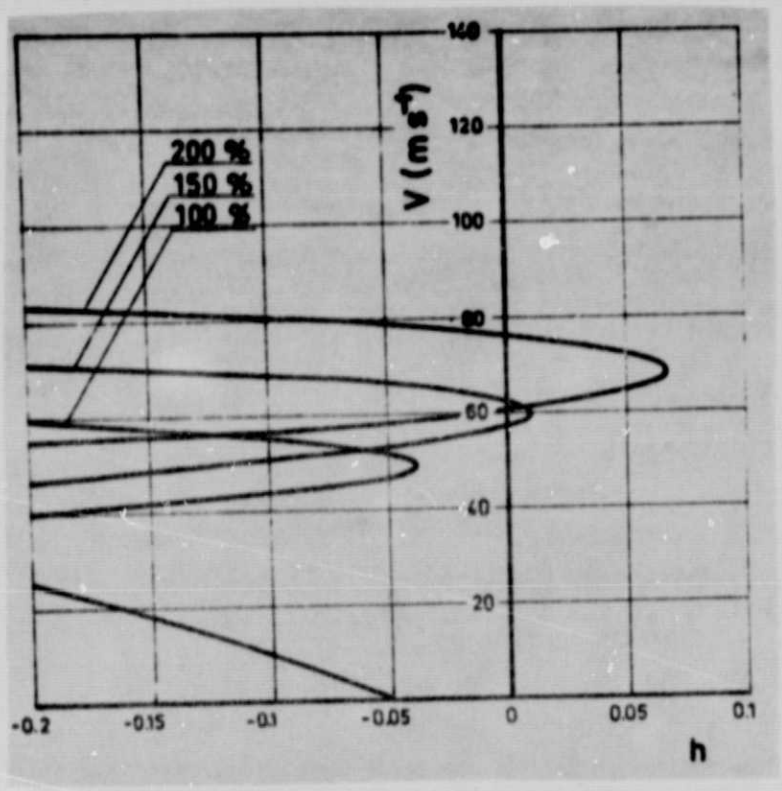

Fig. 12. Damping characteristics for eigen vibration model 8 for a number of values for the aileron moment of inertia, with ballast.

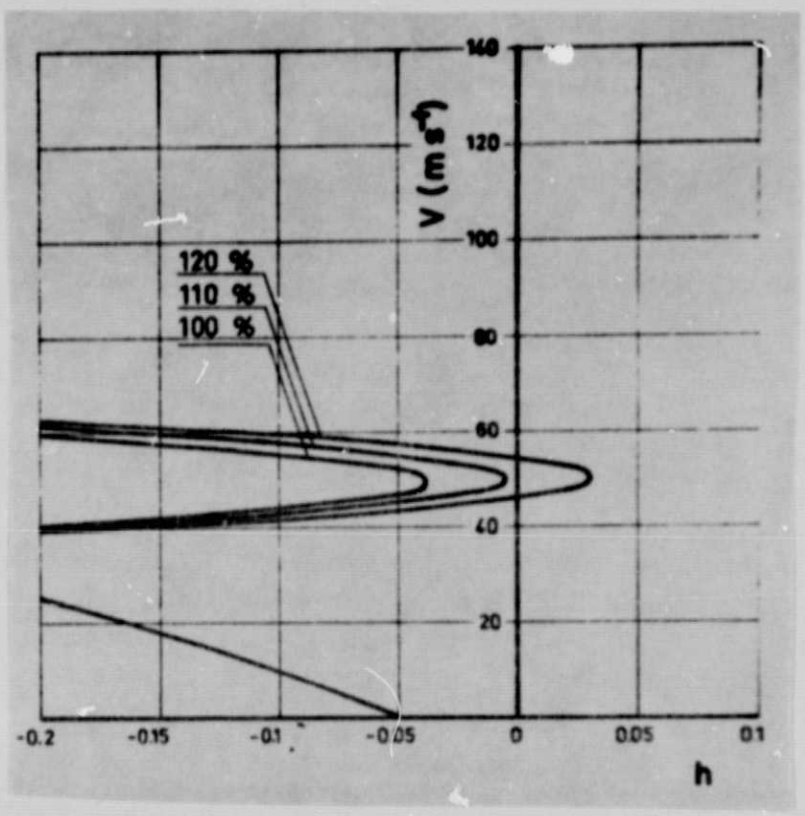

Fig. 13. Damping characteristics for eigen vibration model 8 for a number of values for the static moment of the aileron, with ballast.

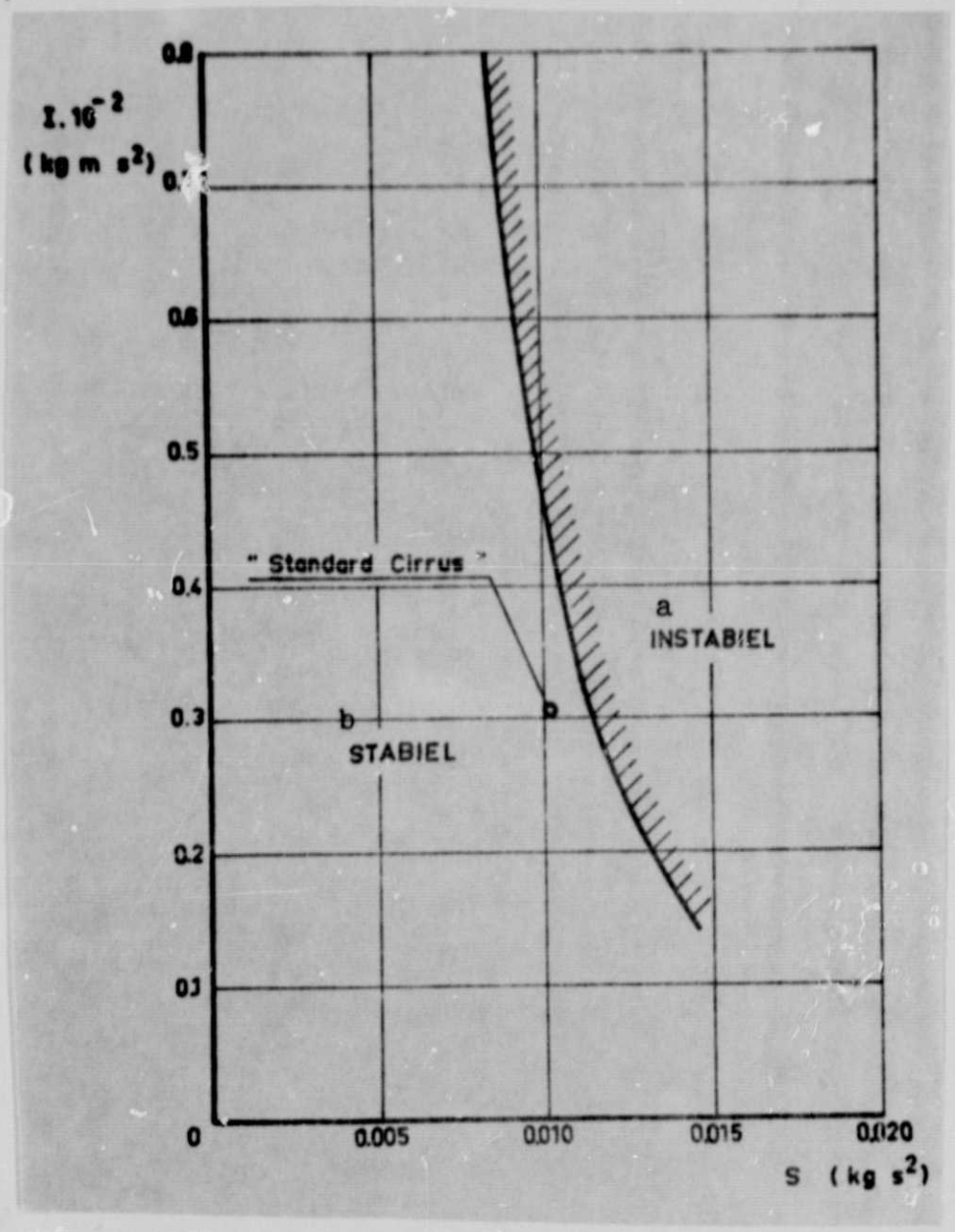

Fig. 14. Stability diagram.

Key: a. Unstable
b. Stable

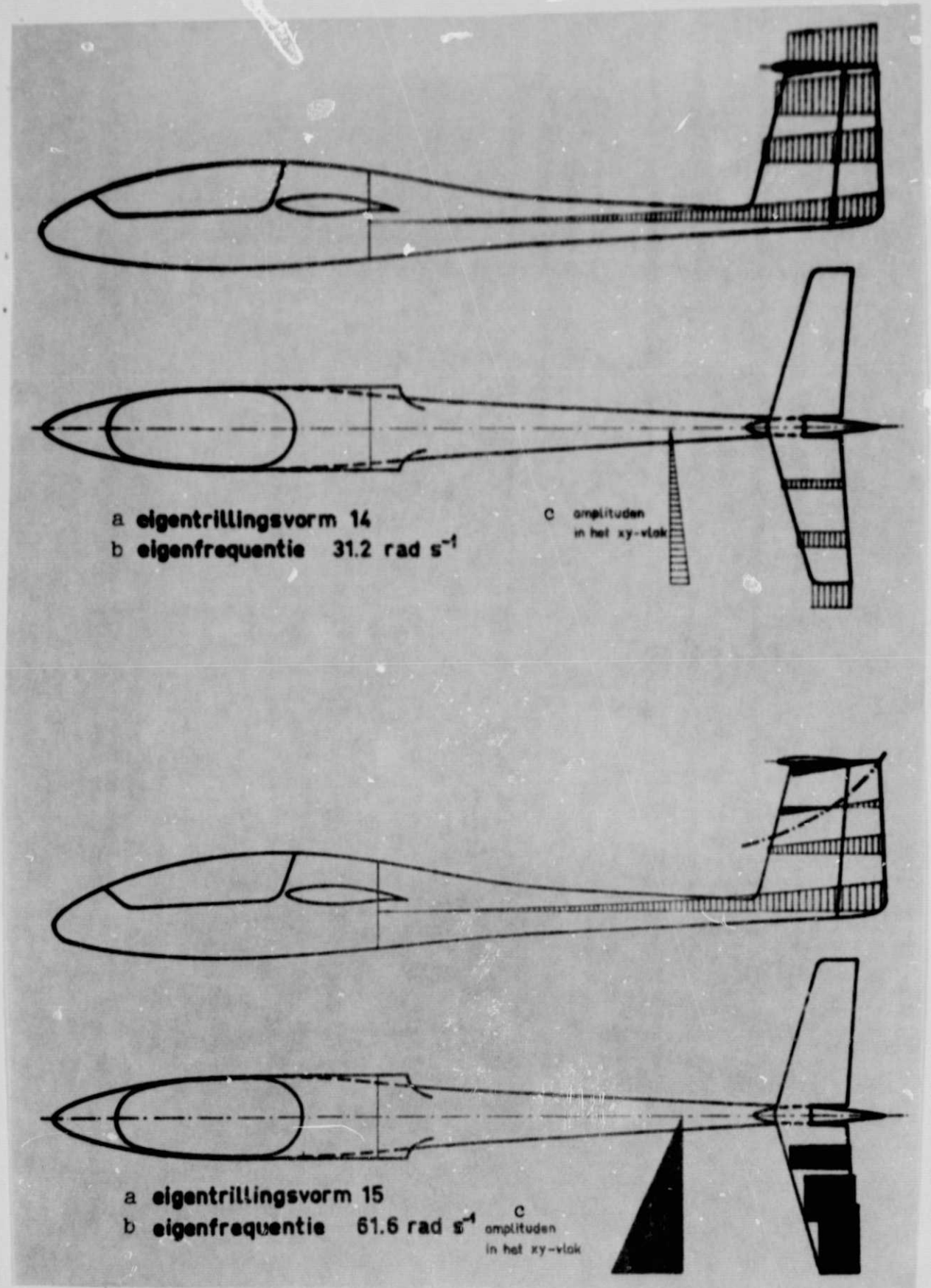

Fig. 15. Asymmetrical vibration models for the rear fuselage with tail surfaces.

Key: a. Eigen vibration model; b. Eigen frequency; c. Amplitude on the xy-surface

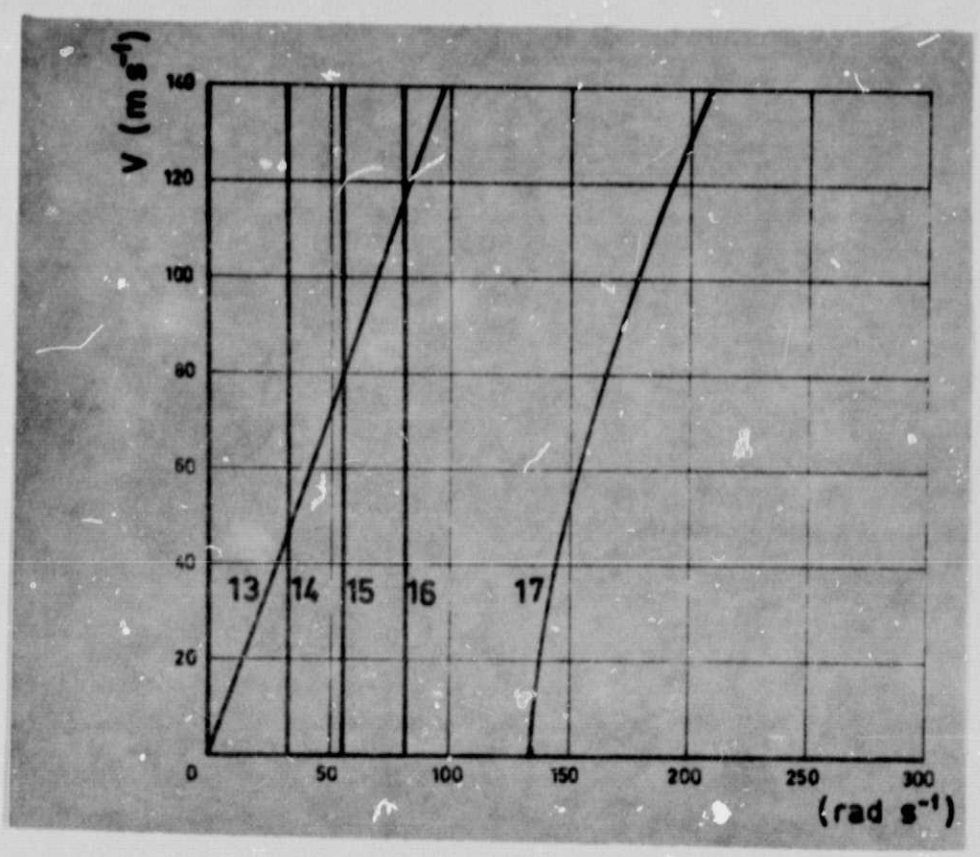

Fig. 16. Curve of the eigen frequencies with flight speed.

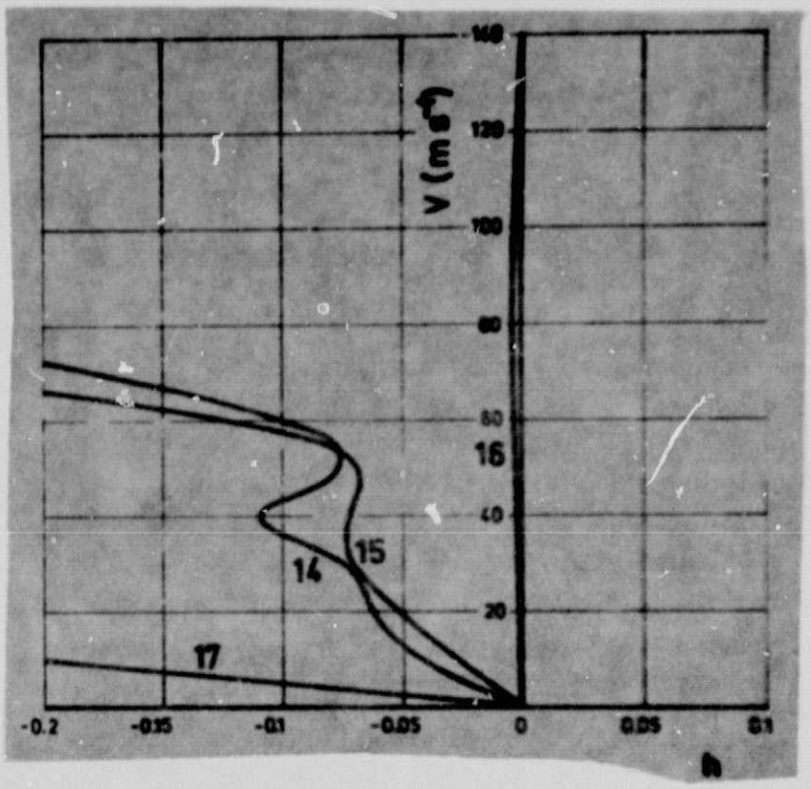

Fig. 17. Curve of damping with flight speed.